FERMILAB-PUB-17-320-TD
ACCEPTED

Development of Low β Single Spoke Resonators for the Front End of the Proton Improvement Plan-II at Fermilab

Mohamed H. Awida, Donato Passarelli, Paolo Berrutti, Ivan Gonin, Sergei Kazakov, Timergali Khabiboulline, Jeremiah Holzabauer, Thomas Nicol, Joseph Ozelis, Mattia Parise, Yuriy Pischalnikov, Oleg Pronitchev, Leonardo Ristori, Gennady Romanov, Allan Rowe, Warren Schappert, Dmitri Sergatskov, Nikolay Solyak, Alexander Sukanov, and Vyacheslav P. Yakovlev

***Abstract*—A total of ten jacketed single spoke resonators type 1 (SSR1) have been fabricated for Fermilab' injection experiment (PIP2IT). PIP2IT is a test bed for Fermilab's future accelerator named proton improvement plan II (PIP-II) that is currently under development. SSR1 cavities operate at 325 MHz to accelerate a proton beam at a relative (to speed of light) velocity (β=0.22). In this paper, we present Fermilab's experience in developing those spoke resonators starting from the design and analysis phase, to fabrication and extensive testing to qualify cavities for cryo-module assembly.**

I. Introduction

PIP-II is a proposed high intensity proton accelerator to be built at Fermilab targeting the intensity frontier with a focus on neutrino experiments. PIP-II could reveal physics phenomena far beyond the energy reach of the Large Hadron Collider, but only in an indirect way [1]. PIP-II is an 800-MeV superconducting linac (SC Linac), constructed of continuous wave (CW) capable accelerating structures and cryomodules, operating with an average H^- beam current of 2 mA and a beam duty factor of 1.1% at a bunch repetition rate of 162.5 MHz. The SC Linac of PIP-II consists of five types of cavities covering beam velocities starting from 11% to 92% the speed of light [2-3], as shown in Fig. 1(a). Cavities will operate at three different frequencies, specifically; 162.5 MHz, 325 MHz, and 650 MHz [3]. The frequencies have been selected as sub-harmonics of the 1300 MHz frequency, commonly used among accelerator community. The superconducting feature of PIP-II's cavities allows the Linac to efficiently operate at a large gradient beyond the limit of normal conducting ones, which shortens the required length of the accelerator. Thus, it saves money on construction cost.

Low β structures, where β is the group of relative velocities of particles to be accelerated, are essential components in any proton or heavy ion particle accelerator as means to get the beam accelerated from a relatively small speed (β ~0.1) to larger values (β ~0.5). Several low β structures have been used before in large scale accelerator projects [4-8]. The structures typically range from drift tubes (DTL), to charged coupled linac (CCL), quarter wave resonators (QWRs), half wave resonators (HWRs), and spoke resonators weather it is single spoke, double spoke, or triple spokes. For instance, the spallation neutron source at Oakridge National Laboratory utilized a DTL in their accelerator to get the beam accelerated right away after the radio frequency quadrupole from 2.5 MeV to 87 MeV, then there is another stage of CCL that takes the beam afterwards from 87 Mev to 186 MeV, where elliptical cavities of relatively high β (0.61, and 0.81) are employed [6]. On the other hand, FRIB utilized two kinds of low β cavities; QWR at 80.5 MHz with β=0.041 and 0.085, and HWR at 322 MHz with β=0.29 and 0.53 [7]. Table 1 summarizes the parameters of several low β cavities that have been used in major particle accelerator projects.

The high intensity goal of PIP-II requires that the Linac operates at an average current of 2 mA, which is problematic as far as beam activation that necessitates a relatively large bore radius for the beam pipe along the accelerator. The RF

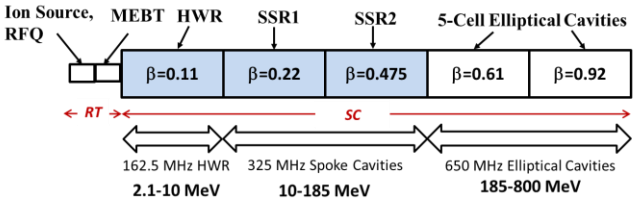

(a)

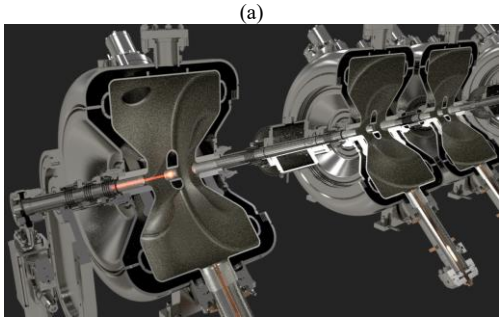

(b)

Fig. 1. Proton improvement plan II (PIP-II) Linac. (a) Linac layout. (b) Virtual picture of single spoke resonator 1 (SSR1) string.

Manuscript received April 28th, 2017. This work was supported by the U.S. Department of Energy, Operated by Fermi Research Alliance, LLC, under Contract DE-AC02-07CH11359 with the U.S. DOE.

Authors are with the Fermi National Laboratory, Batavia, IL 60510 USA 630-840-3935; e-mail: mhassan@fnal.gov.

Table 1. Low β cavities in major particle accelerator projects.

Project	Cavity Type	Freq [MHz]	β	Voltage Gain [MV]	Ref
PIP-II	HWR	162.5	0.11	2.00	[4]
	SSR1	325	0.22	2.05	[5]
	SSR2	325	0.475	5.00	[3]
SNS	DTL	402.5	0.073-0.403	3.00	[6]
	CCL	805	0.403-0.550	1.72	
FRIB	QWR1	80.5	0.041	0.81	[7]
	QWR2	80.5	0.085	1.80	
	HWR1	322	0.29	2.10	
	HWR2	322	0.539	3.70	
ISAC-II	QWR	106	0.057, 0.071	1.10	[8]
	QWR	141	0.011	1.10	

design of cavities given the beam pipe size requirements is quite challenging.

The pulsed mode of operation for PIP-II mandates addressing Lorentz Force Detuning (LFD) during the mechanical design of cavities in its Linac, while to be compatible with CW operation, frequency sensitivity to pressure fluctuation in helium bath needs also to be minimized.

Spoke cavities were chosen for PIP-II Linac to accelerate the H^- beam from 10 MeV to 185 MeV. A single spoke design was selected over multiple spokes to widen the range of β the cavity can be utilized for in beam acceleration [2-4]. Also, the spokes are more favorable over HWRs at relatively higher frequencies because it is more manageable to frequency scaling while the HWR will get shorter at higher frequencies. Two stages of single spoke cavities namely; SSR1 with β=0.22, and SSR2 with β=0.475, are utilized in the reference design of PIP-II [2-3]. Two cryomodules of SSR1 are needed to adequately accelerate the beam before moving to the next section of SSR2 cryomodules. In that perspective, ten cavities of SSR1 were fabricated and 'vertically' tested to build the first cryomodule of SSR1.

This paper is organized as follows: in Section II the electromagnetic design of the cavity is described, while the structural design is addressed in Section III. In Section IV the system design is presented, then the fabrication and quality control process is described in Section V. The preparation and processing before testing is explained in Section VI, followed by testing and qualification in Section VII, and finally concluding in Section VIII.

II. RF Design

SSR1, shown in Fig. 2, is a single spoke resonator. We have used the eigenmode solver of CST Microwave Studio [9] to design and optimize the RF volume of the cavity. Table 2 lists the RF requirements for SSR1 and constraints on its geometry. For instance, the cavity diameter is required to be less than 0.5 m. Also, the frequency of the cavity was chosen to be 325 MHz, as a subharmonic of the commonly used 1300 MHz. The bandwidth of the cavity is expected to be 90 Hz given a quality

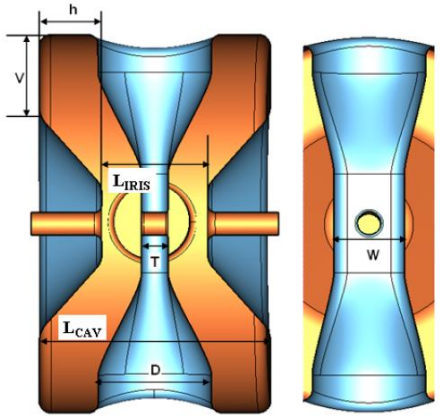

Fig. 2. Cross section of the SSR1 with the main parameters used in the optimization process

Table 2. RF Requirments on SSR1.

Parameter	Requirement
Frequency	325 MHz
Shape	Single Spoke Resonator
β_g, β_{opt}	0.215, 0.22
E_{acc}	10 MV/m
Iris aperture	30 mm
Inside diameter	492 mm
Bandwidth (f_0/Q)	90 Hz
E_p	<40 MV/m
B_p	<70 mT

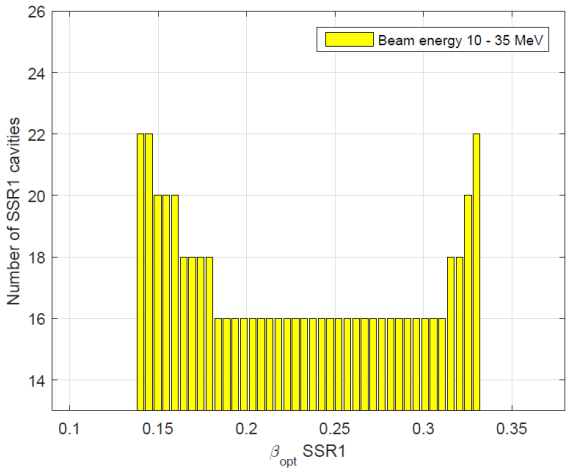

Fig. 3. Number of SSR1 cavities for PIP-II as a function of β_{opt}.

factor of 10^6. Meanwhile, the cavity is required to achieve an accelerating gradient E_{acc} of 10 MV/m, which translates to a voltage gain per cavity of 2.0 MV, given an effective length ($L_{eff}= \beta_0\lambda$) of 203 mm.

Studies of beam dynamics dictated the beam aperture to be of 30 mm in radius. Meanwhile, the number of cavities needed to achieve the final energy was calculated as a function of the cavity optimum group velocity β_o. The beam dynamic simulations take into account the cavity transit time factor, peak fields and a simple phase advance profile for SSR1. Figure 3 illustrates the number of SSR1 cavities needed to accelerate the beam from 10 MeV to 35 MeV versus the optimum group velocity; β_{opt}. To minimize the number of cavities, β_{opt} can be anywhere from 0.18 to 0.31. We have

chosen to design the cavity with a β_{opt} of 0.22 value as a compromise to reduce the cavity effective length.

Meanwhile, the peak surface magnetic and electric field are required to be less than 70 mT, and 40 MV/m to avoid magnetic quench and radiation due to field emission, respectively.

a) Electromagnetic Design and Optimization

The geometry of the SSR1 is relatively complicated. The main geometrical parameters were only used for optimizing the structure, which include: L_{cav} the cavity length (end-wall to end-wall along beam axis), L_{iris} the iris to iris length, D the spoke base diameter, W the spoke width, T the inner electrode thickness, h and v the cylindrical shell and end-wall dimensions, respectively as depicted in Fig. 2.

In the optimization process, the iris-to-iris distance (L_{iris}) was kept equal to 2/3 of the effective length of the cavity (L_{eff}), while all other parameters as introduced above were changed to optimize the EM performance of the resonator.

In fact, the minimization of the peak surface electric field (E_p) involved mainly the following parameters W, T and L_{iris}, since these parameters define the geometry in the region of high electric field nearby the iris. Figure 4 shows the optimization process of E_p, where E_p/E_{acc} and R/Q are plotted versus W, and T/L_{iris}, in (a), and (b), respectively. In fact, Ep/E_{acc} has a minimum at a spoke width W of 120 mm, and a T/L_{iris} of 0.31. On the other hand, the ratio D/L_{cav}, and the end cup profile dimensions were optimized to achieve a low peak magnetic field. The results of the simulations are shown in Fig. 5. The B_p/E_{acc} has a minimum at D/L_{cav} of 0.49.

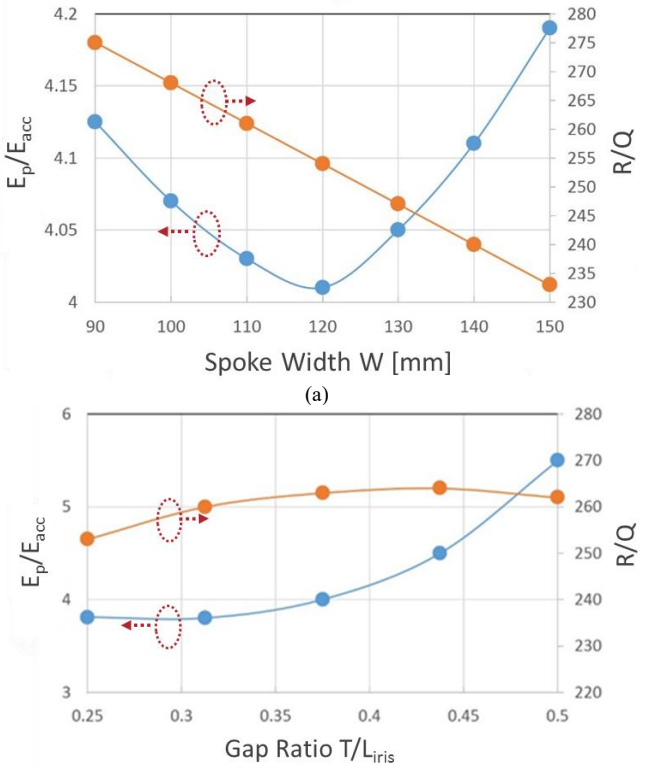

Fig. 4. RF optimization of SSR1's axial region. (a) E_p/E_{acc} and R/Q vs. W. (b) E_p/E_{acc} and R/Q vs. T/L_{iris}.

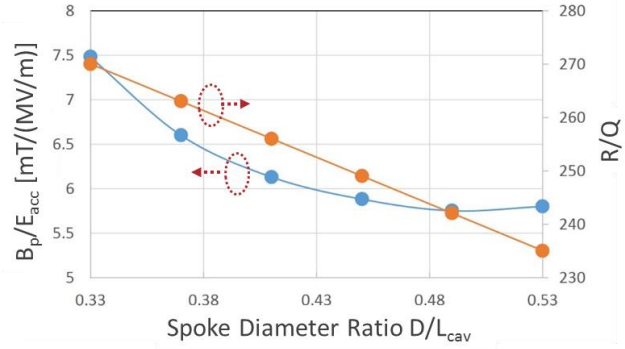

Fig. 5. RF optimization of SSR1's peripheral region illustrating B_p/E_{acc} and R/Q vs. D/L_{cav}.

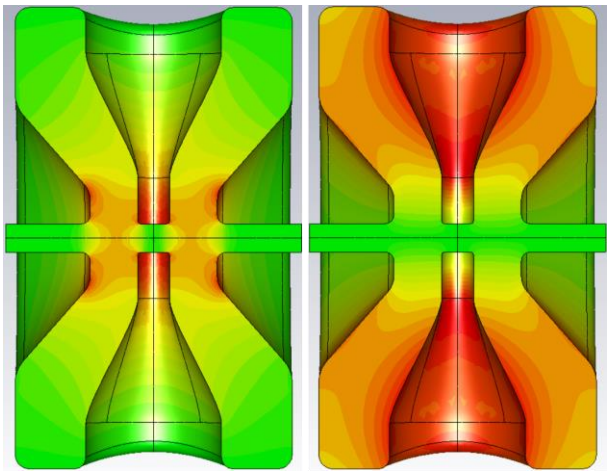

Fig. 6. Electromagnetic field of SSR1. (a) Electric field. (b) Magnetic field. The field strength increases as the color changes from green to yellow to red.

Table 3. RF Performance of Optimized SSR1.

Parameter	Performance
Ep/Eacc	3.84
Bp/Eacc	5.81 mT/(MV/m)
G	84 Ω
R/Q	242 Ω

The electric and magnetic fields of the optimized geometry are shown in Fig. 6. The final EM parameters are summarized in Table 3. The optimized cavity has R/Q of 242 Ω with Ep/E_{acc} of 3.84 and B_p/E_{acc} of 5.81, corresponding to 38.4 MV/m and 58.1 mT projected peak surface electric and magnetic fields, respectively at 10 MV/m accelerating gradient.

b) Multipacting Analysis

Multipacting (MP) is a common problem for low beta superconducting spoke cavities [10-11]. In such structures, strong electron activity occurs at certain electric field gradients. New advanced computing capabilities make it possible to simulate particle dynamic in the realistic 3D electromagnetic fields of the cavity [9].

The MP in SSR1 is, in fact, a mix of different particle dynamics modes, specifically, one point non-resonant, one-point resonant, and two-point resonant MP modes.

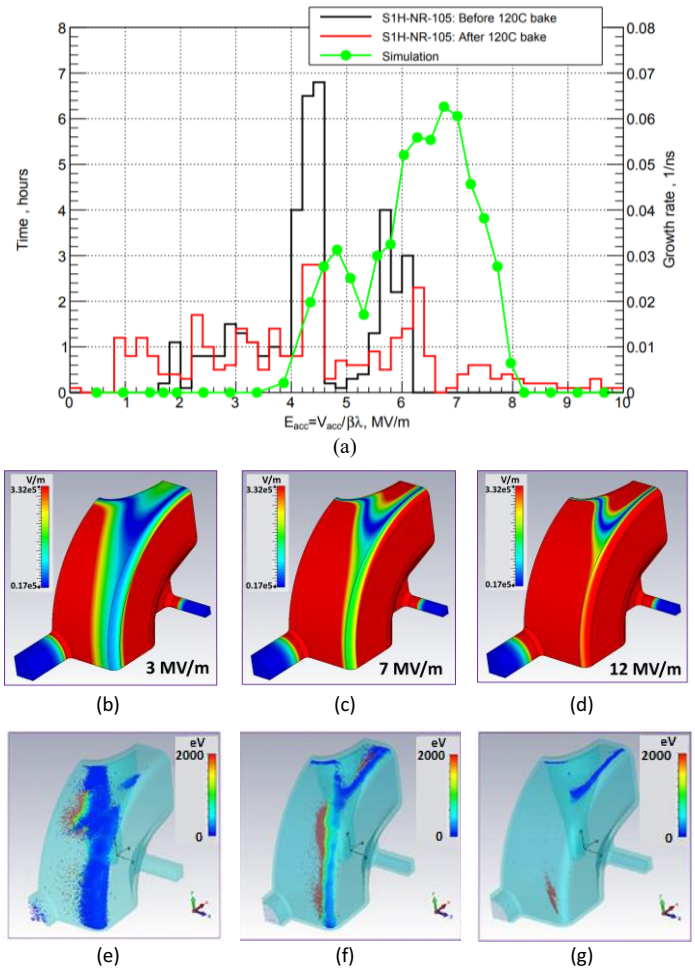

Fig. 7. Multipacting analysis of SSR1. (a) Simulated growth rate and measured MP processing time versus gradient. Electric field at (b) 3 MV/m, (c) 7 MV/m, and (d) 12 MV/m. Particle tracing at (e) 3 MV/m, (f) 7 MV/m, and (g) 12 MV/m.

Each of the modes dominates at certain levels of RF fields. As a result, we can see in practice and in the simulations three major barriers of MP, as shown in Fig. 7(a). The first barrier starts at an accelerating gradient of about 2 MV/m and is associated mostly with non-resonant MP. Typically, this 2 MV/m barrier can be passed quickly during testing. On the other hand, the one-point resonant MP dominates in the second barrier that starts at about 4 MV/m. This barrier is relatively stubborn one and it takes approximately 8 hours or 30 hours of RF conditioning to pass it through with and without 120 °C baking, respectively as shown in Fig. 7(a). The third barrier exists at 6 MV/m and it is dominated by a two-point resonant MP in the cavity corners. This kind of MP is the most "critical" one (as it is close to the gradient of operation), but due to the small area of development the total emission current is not very high and RF conditioning is somewhat faster than it is for the second barrier. Afterwards, the area with the conditions favorable for MP continue shrinking with increasing RF fields and gradually the intensity of MP drops to almost zero nearby the 10 MV/m gradient of operation, as shown in Fig. 7(a).

The MP areas with a corresponding surface electric field are shown at different accelerating gradients in Fig. 7(b), (c), and (d) for gradients 3, 7 and 12 MV/m, respectively. It is clear that the MP areas occupy a significant portion of the cavity surface and exist from very low fields up to a relatively high accelerating gradient of 12 MV/m. However, the MP activity appears to be localized on vulnerable surfaces where the MP condition is favorable as shown in Fig. 7(e)-(g). In fact, the extensive simulations with CST Particle Studio show that the most intensive spot of MP migrates from one spot to another with an accelerating gradient increase, as shown in Fig. 7(e), (f), and (g), for gradients 3, 7, and 12 MV/m, respectively.

Moving to new areas lets the MP sees "fresh" unconditioned parts of the surface. We think, that this migration of the MP location is a reason for the broad interval of MP.

The broad band characteristic of the MP in SSR1s is a concerning issue particularly for testing since multiple MP levels lengthen the RF conditioning process. In some cases, it took several days to process the barrier at 4 MV/m. However, we believe that there was some residual water after the 120 °C that increased the MP activity. Proper 120 °C baking for at least 48 hours helps to reduce the conditioning process as demonstrated in Fig. 7(a) in case of Cavity #105 [12-13].

c) HOM Analysis and Measurements

Higher Order Mode (HOM) analysis was carried out on SSR1 to investigate the risk of HOM, as modes with significant shunt impedance can cause beam instabilities [14]. HOM measurements have been taken as well on several spoke cavities, including the harmonic response and the bead pull measurements.

Given the cavity geometry and its symmetry, it is possible to divide HOMs in three kinds namely: monopoles, dipoles, and quadrupoles. One can calculate one kind of HOMs by enforcing proper boundary conditions on the two symmetry planes (perfect electric conductor "PEC", and perfect magnetic conductor "PMC") as follows: PMC-PMC for monopoles, PMC-PEC/PEC-PMC for both horizontal and vertical dipoles, and PEC-PEC for quadrupoles.

Figure 8 shows the results of the HOM analysis. The measured and calculated R/Q values for the monopoles versus frequency are shown in Fig. 8(a). Simulated R/Q of the fundamental mode at 325 MHz frequency is 239 Ω, while all other HOM monopoles are less than 1 Ω in R/Q (at β=0.22) with the largest value being 0.61 Ω at 921 MHz. Bead pull measurements were carried out on several fabricated cavities, measuring the monopoles up to 2 GHz, as shown in Fig. 8(a). R/Q of the fundamental mode for the different measured cavities is in good agreement with the simulated value. Relatively larger spread exists in the measured R/Q values for the HOMs, which is expected, as HOM fields are quite smaller near the cavity axes, thus closer to the noise level. The measured R/Q of the HOM monopoles is less than 1 Ω. It is worth mentioning also that the measured frequency spread of the fabricated spoke cavities from their average values for monopole frequencies is less than 7 MHz.

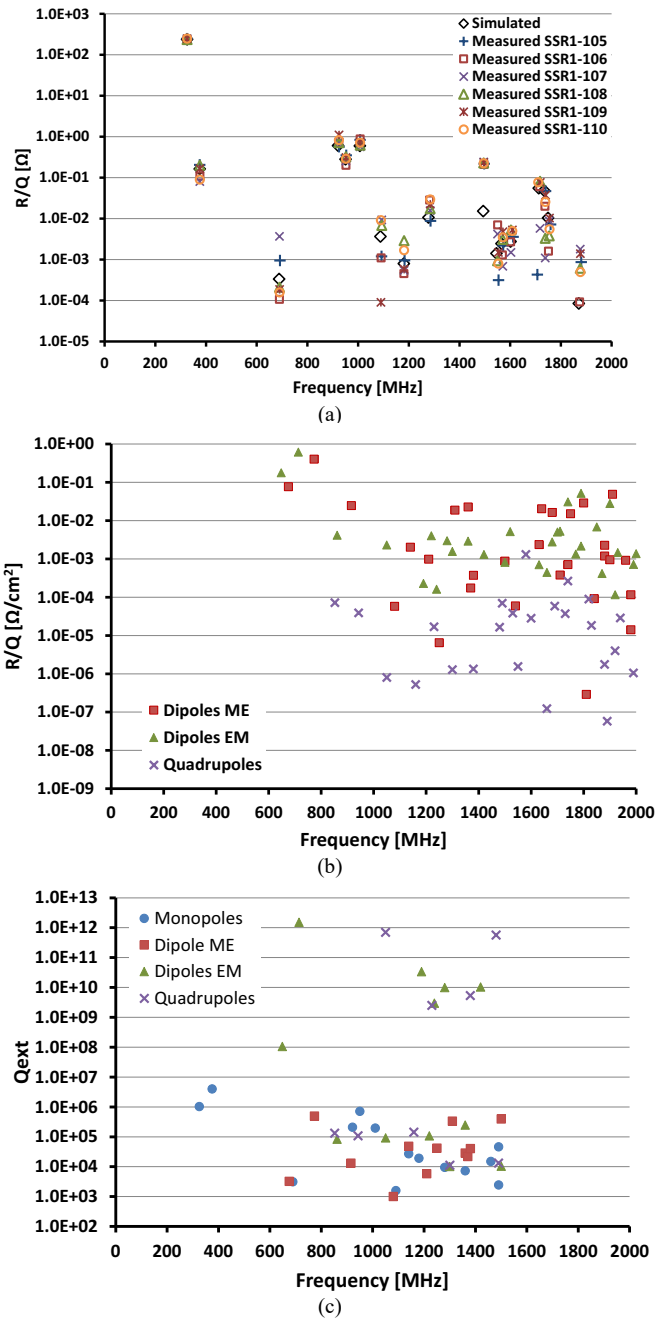

Fig. 8. Higher order mode (HOM) analysis of SSR1. (a) Measured versus simulated R/Q for the monopoles. (b) Simulated R/Q of the dipoles and quadrupoles at β=0.22. (c) Simulated Q_{ext}.

Figure 8(b) shows the calculated R/Q in Ω/cm² for the dipoles and quadrupoles. For the dipoles, all of them are less than 1 Ω/cm² in R/Q with the largest mode being dipole EM at 713 MHz with R/Q equals 0.6 Ω/cm². On the other hand, all the HOM quadrupoles are less than 0.01 Ω/cm² with the largest mode being at 1580 MHz with R/Q equals 0.0013 Ω/cm².

External quality factor for all the modes has been calculated assuming 50 Ω coupler port with inner conductor of 33.4 mm in diameter. The depth of the coupler probe antenna was adjusted to have Q_{ext} of the fundamental mode equal to 10^6. Figure 8(c) shows the simulated Q_{ext} values of all the HOMs versus frequency. Largest Qext is that of the dipole EM mode at 713 MHz being ~10^{12}.

The spectrum of monopoles in SSR1 cavities is quite sparse as shown in Fig. 8(a). Moreover, the mode impedance, and (R/Q), falls quickly with frequency. Shunt impedance is of the order of a few mΩ at about 2 GHz. In fact, the probability to encounter losses above 10 μW is less than 0.5% [15]. Therefore, HOM dampers are not needed for SSR1 cavities.

d) Kick Analysis and Multipole Effects

Transverse kicks can occur in SSR1 cavities due to geometrical variations of the fabricated cavities. From our fabrication experience, three deviations are of concern; beam pipe and spoke shifts in transverse direction, and spoke shift in longitudinal direction [16]. A simulation study was carried out while artificially implementing these variations in the simulation model as listed in Table 4. The transverse spoke shifts, whether it is in x (along the spoke), or y (perpendicular to the spoke) direction produces more transverse kick rather than the pipe shift or the longitudinal shift of the spoke.

Bead-pull measurements were also conducted to evaluate the transverse kick values in some of the fabricated cavities as shown in Table 4. It is worth noting here, that the fabricated cavities have combined various deviations leading to the kick values listed in the Table, but these values agree with the physical dimension measurement that each cavity undergoes using coordinate measuring machines (CMM). Maximum kick in the fabricated cavities is within 154 keV, which can induce about 1.12 mrad beam deviation, but this deviation can be corrected with the 10 mrad specified correctors of PIP-II [3].

On the other hand, since SSR1 geometry has a central electrode (spoke) that lies on one of the axes perpendicular to the particles motion, the spoke breaks axial symmetry of the cavity. This asymmetry violation reflects on the transverse EM field components giving a quadrupole field perturbation, which affects the particle transverse dynamic [17]. We have investigated this field perturbation, that is commonly called "Multipole Effect", and it is worth mentioning here the multipole effect in SSR1 is very small and it can be easily managed again by the 10 mrad corrector inside the cryomodule.

Table 4. Simulated and Measured Transverse Kick Due to Various Geometrical Variations (in keV for 2 MeV energy gain per cavity).

		$\lvert\Delta P_x.c\rvert$	$\lvert\Delta P_y.c\rvert$
Simulated Deviations	Beam Pipe 1mm Shift in y	~0	57.2
	Spoke 1 mm Shift in x	83.3	~0
	Spoke 1 mm Shift in y	~0	101.7
	Spoke 1 mm Shift in z	~0	~0
Measured SSR1	105	36.6	15.2
	106	3.5	24
	107	25.6	1.3
	108	105.7	3.2
	109	40.1	154.3
	110	0.6	72.6

III. Structural Design

The jacketed SSR1 cavity consists of two nested cryogenic pressure vessels operating at 2 K: the inner vessel is the bare superconducting SSR1 cavity and the outermost vessel is the helium containment (or helium) vessel, see Fig. 9. Table 5 lists the mechanical and frequency sensitivity requirements on the cavity geometry. The cavity must withstand a maximum allowable pressure of 2 bar, 4 bar at room temperature and 2 K, respectively. Meanwhile, the frequency sensitivity to pressure fluctuations *df/dP* shouldn't exceed 19 Hz/mbar. Also, *LFD* coefficient should be minimized to better than 5 Hz/(MV/m)^2. In this section, we will discuss the structural analyses we performed to reach the final structural design of the cavity.

a) Bare Cavity

The bare cavity is made from a 3mm niobium sheet that strictly follows the RF domain. The cavity shell is then structurally reinforced by adding several stiffening features, as shown in Fig. 10(a). Specifically, daisy, donut and circumferential ribs are added to reinforce the cavity shell. In fact, the bare cavity is required to withstand a maximum allowable pressure (MAWP) of 2 bar at 2 K during vertical testing. Moreover, frequency sensitivity to pressure fluctuation (*df/dP*), and *LFD* coefficient need to be minimized. All these requirements necessitate stiffening of the structure. Figure (b) and (c) illustrate the von mises stresses on the cavity under 2 bar of pressure load with and without the stiffening features, respectively. Clearly, the stiffening features, especially the donut ribs significantly reduce the stresses on the corners of end walls from 570 MPa to 140 MPa and being localized at the donut rib to the cavity, which makes it not of a concern because it is below the allowable stress of niobium at 2 K (171 MPa) [18].

Fig. 9. Structural geometry of SSR1 with a cut showing the niobium bare cavity and the helium vessel.

Table 5. Mechanical and Frequency Senstivity Requirments on SSR1.

Parameter	Requirement
Operating temperature	1.8-2.1 K
MAWP	2 bar (RT), 4 bar (2K)
Sensitivity to pressure *df/dP*	<19 Hz/mbar
- LFD coefficient, - *df/dE*^{2}	< 5 Hz/(MV/m)^2

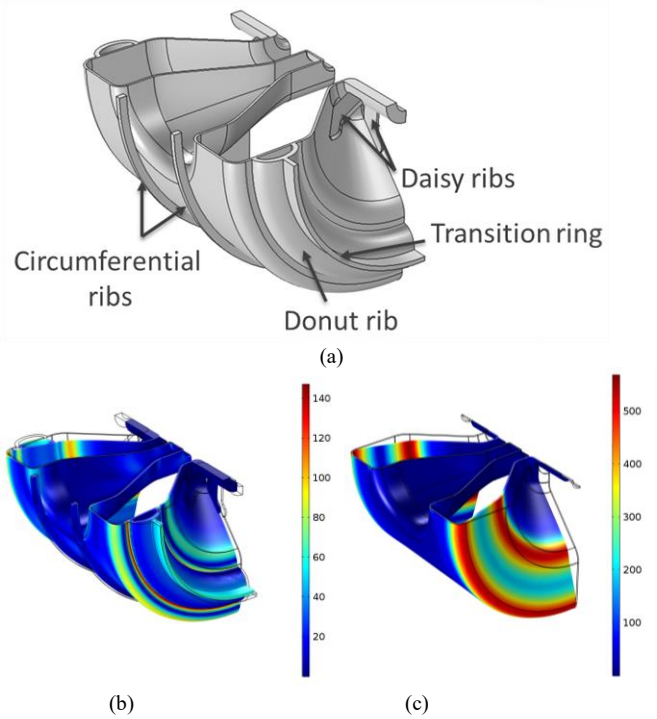

Fig. 10. Results of linear elastic FE analysis of the niobium cavity in the load case of P=2 bar. (a) Cavity shell with stiffening features. (b) Stress on the niobium shell with stiffening features. (c) Stress on the niobium shell without stiffening features.

On the other hand, a transition ring is used to couple the bare cavity to the helium vessel. It helped in the process of reducing the RF frequency sensitivity to helium pressure fluctuations as will be discussed later.

b) Jacketed Cavity

Many aspects need to be considered during the structural design of a cavity, and often compromises must be found to satisfy all the functional requirements. The structure of SSR1 cavities was designed to mitigate the effects of microphonics and Lorentz force detuning, and meet the requirement of ASME BPVC Code at the greatest extent possible [18].

The typical operating temperature for SSR1 cavities is in the range from 1.8 K to 2.1 K. At this temperature range a bath of superfluid helium confined by the helium vessel and surrounding the cavity exerts a pressure (20-30 mbar) on both vessel and cavity niobium shell, while the RF volume of the cavity is pumped down to ultra-high vacuum, and the entire jacketed cavity is placed in a cryostat under insulating vacuum. At nominal operating conditions, there is a marginal force on the cavity structure. However, an accidental loss of vacuum would result in very rapid boiling of the helium, causing a consequent pressurization of the helium space. This risk is the driver for the pressure load specifications on the cavity structure.

The differential pressure can be detected between the volumes defined by cavity and helium vessel during the first phases of operation before the cooldown. A relief valve setting of 0.2 MPa is needed to ensure the cavity is protected during cool down, testing, and warming up. But again, since the yield strength of niobium and stainless steel improves significantly

at cryogenic temperatures, two ratings are allowed for the maximum allowable pressure for the dressed cavity; one at room temperature and one at cryogenic temperatures. A higher rating at cryogenic temperatures allows the system piping to be sized for higher short-term pressure increases which can occur in the event of vacuum loss in cavity or insulating vacuum while the cavity is cold. Therefore, the jacketed SSR1 cavity must satisfy two values of maximum allowable working pressure (MAWP), 2 bar at 293 K when the niobium material strength is low, and 4 bar at 2 K when the niobium strength is significantly higher.

The final validation of structural design of the jacketed SSR1 cavity was made using the rules of ASME BPVC, Section VIII, Div. 2. Some of the most common non-compliances were addressed using "equivalent rules" in terms of safety, when the Code does not apply [18].

The geometries of the structures and loading conditions of SRF cavities, and therefore the stress distributions, are often complicated and do not lend themselves entirely to design by design-by-rules method. The design-by-analysis method can be used to optimize those features not amenable to design-by-rules method. Design-by-analysis method assumes a numerical analysis technique will be used, and either elastic or elastic-plastic analysis is permitted.

In the case of the SSR1, ANSYS structural analysis software [19] was used to perform the finite element analyses and provide protection against the most critical mode of failure for this type of structures; the plastic collapse. The analysis for this failure mode focuses on the internal pressure of the vessel and prevents plastic instability, ensuring that the pressure vessel does not experience plastic deformation that may lead to collapse. Moreover, the analysis avoids unbound displacement in each cross-section of the structure.

Elastic plastic analyses were performed for several load cases while combining both the pressure and the dead weight (1250 N) of the cavity at both room temperature and at 2 K. In each case, the pressure was applied, and increased incrementally until collapse (i.e., failure of the finite element model to converge) occurred.

Figure 11 shows the location where the most critical failure mode, so-called plastic collapse, for this type of structures would initiate in the SSR1 system of vessels. The niobium structure starts to show evidences of plastic collapse at a value of pressure of 2.44 bar (0.244 MPa), when at room temperature and it is subject to the loading case: pressure and dead weight. However, the pressure that would lead to failure is higher than the required MAWP of 2 bar at 293 K (0.2 MPa).

Similar analysis was carried out at 2 K. In this case, the collapse pressure was found to be 8.97 bar (0.897 MPa), which is again higher than the MAWP of 4 bar (0.4 MPs) at 2 K.

In conclusion, the jacketed SSR1 cavity represents a sound mechanical structure that poses no hazard to personnel or equipment because the values of MAWPs required have been demonstrated to be below the critical values that would initiate any of the failure modes.

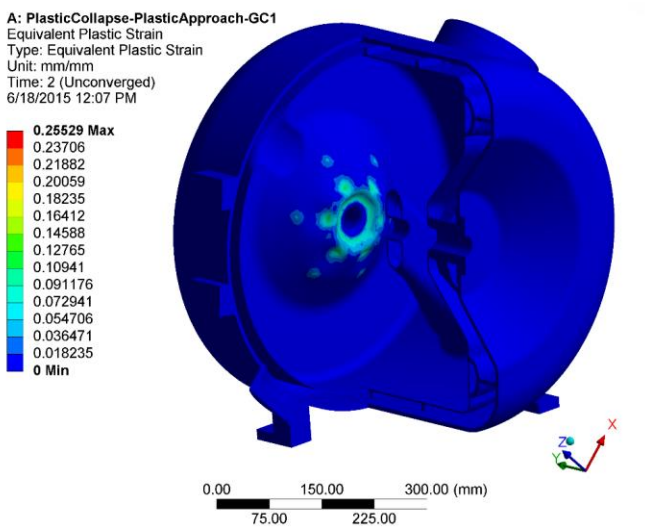

Fig. 11. Results of elastic plastic stress analysis under the load case of both pressure and dead weight (1250 N) at room temperature. The highlighted area is the location where the failure initiates under 2.44 bar collapse pressure, which is exceeding the value of MAWP (2 bar) at room temperature.

IV. System Design

In this section the system design and analysis of SSR1 is described, in particular the overall system performance, the tuning mechanism, and analysis to minimize frequency detuning weather it is because of pressure fluctuations or Lorentz force detuning. We present also in the section other peripheral devices needed to operate the cavity including low and high power couplers.

a) Low Power Coupler

During vertical testing where the cavity is close to being critically coupled, a low power coupler that is simply a 50 Ω coaxial line feeding an antenna of diameter 12.7 mm was used. The length of the antenna is determined to have a Q_{ext} of $2x10^9$, which is suitable to secure the required critical coupling to the cavity.

b) High Power Coupler

The cavity needs to be tested while it is over-coupled, similar to its actual operating conditions with the beam. A high-power coupler is needed for this. In fact, the beam power gain per cavity under CW is 2 kW, while the maximum design power (PIP-II, 5 mA) is 30 kW. Therefore, the high-power coupler is designed to sustain a 30 kW of CW RF power at 325 MHz.

The geometry of the coupler [20-21] and its constituting parts is shown in Fig. 12(a). One ceramic window is used at room temperature with no external adjustment, which simplifies the coupler geometry. The coupler features also an air-cooled center conductor.

Three prototype couplers have been fabricated and were successfully tested up to 8.5 kW (CW) at room temperature. Figure 12(b) shows the manufactured cold-end assembly of one of the three prototype couplers.

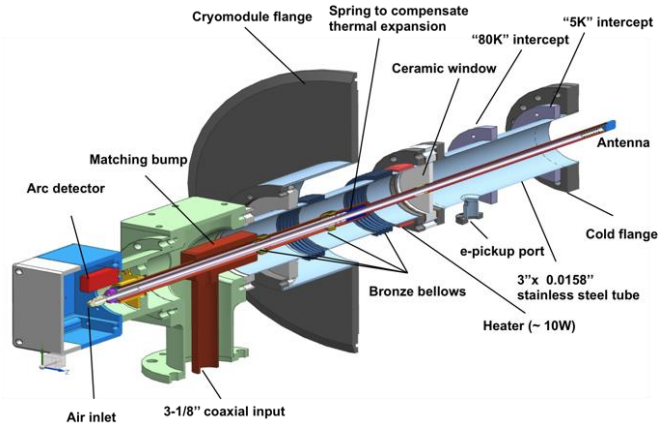

(a)

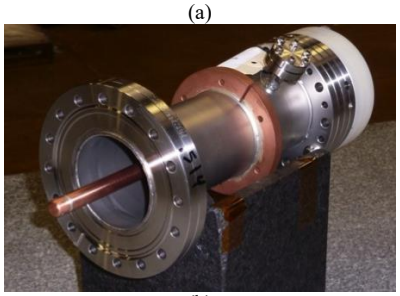

Cold-end assembly

(b)

Fig. 12. High power coupler of SSR1 for testing the cavity under over coupling condition. (a) Coupler different parts. (b) Manufactured cold-end assembly

One of the three couplers was tested at the maximum design power of 30 kW in CW mode. A total of ten production couplers (cold-ends) are under development.

The high-power couplers are attached to the spoke cavities during testing and qualification before qualifying cavities for string assembly. It is worth mentioning here that the cold-end of the couplers is assembled on each cavity in a class 10 cleanroom using a specific custom-made tool and careful procedure to maintain a "particle-free installation".

c) Frequency Tuning Mechanism

Frequency tuning of SRF cavities is essential to precisely bring the cavity to the targeted frequency of operation at 2 K. In addition, the capability of detuning the cavity off resonance is essential for machine operation in case something went wrong with a specific cavity or a cryomodule.

Both coarse and fine tuning mechanisms are needed for SSR1, such that a tuning range of 135 kHz, and 1 kHz are provided by the coarse and fine tuning mechanisms, respectively. The coarse tuning is achieved through a specially designed lever tuner [22], as shown in Fig 13(a), and (b). The tuner is a double lever system made of stainless steel alloy; SS316L. A schematic representation of the tuning mechanism is depicted in Fig. 13(a), illustrating the two arms of the tuner, namely; main arm that goes along the cavity and a secondary arm that connects to the motor. Meanwhile, the fine tuning is provided by Piezos actuated by motors in series, as illustrated in Fig. 13(a) and (b). A 3D model of the tuner assembled on cavity is shown in Fig. 13(c).

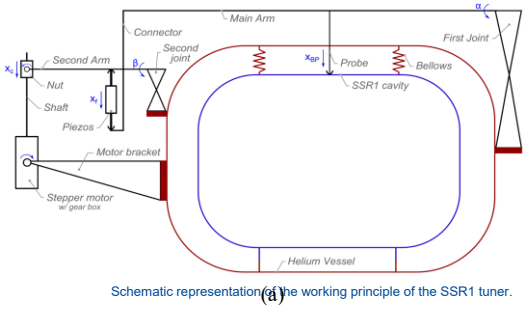

Schematic representation of the working principle of the SSR1 tuner.

(a)

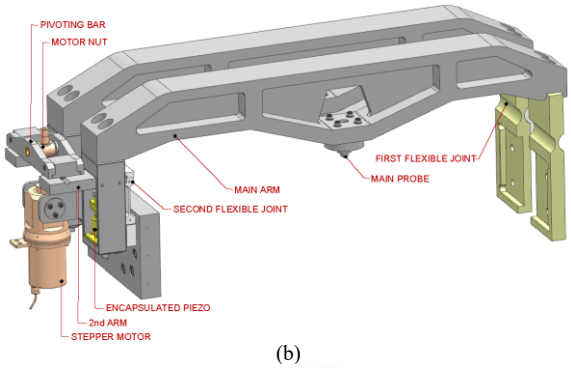

(b)

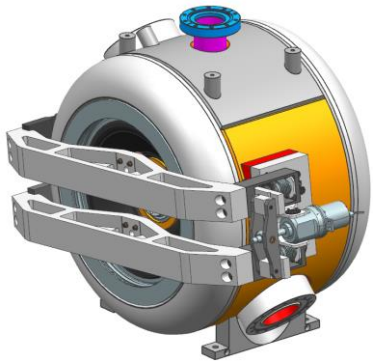

(c)

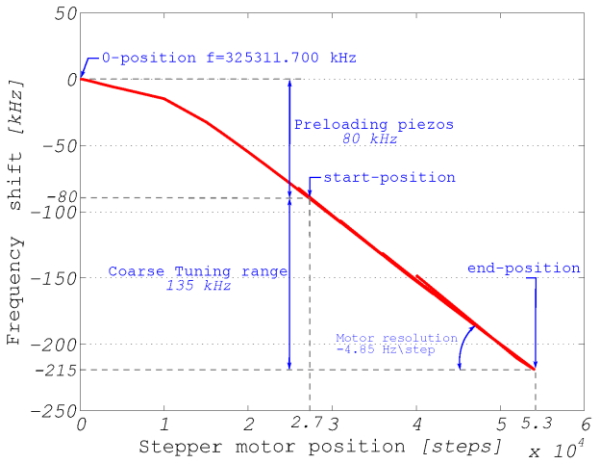

(d)

Fig. 13. Tuner of SSR1 (a) Schematic representation of the tuning mechanism. (b) 3D model of tuner. (c) 3D model of the tuner assembled on cavity. (d) Tuner testing during integrated test.

A prototype version of the tuner was tested at the Spoke Test Stand (STC) during an integrated test. Figure 13(d) demonstrates the frequency shift in kHz versus the stepper motor position. During piezo preloading the cavity frequency

was changed by -80 kHz, then the tuner successfully provided the required 135 kHz tuning range.

d) Frequency Detuning and Sensitivity Coefficients

Superconducting cavities are hypersensitive to frequency fluctuations as any minor drift (few tens of Hz) in the operating frequency would get the cavity seriously detuned. Frequency detuning is mainly caused by either the fluctuations in the applied Helium bath pressure, by the radiation pressure of the electromagnetic field inside the cavity, or by mechanical modes [23]. Conventionally, the cavity sensitivity to pressure fluctuation is expressed by the sensitivity coefficient *df/dP*, while the frequency detuning due to radiation pressure is quantified by the Lorentz Force Detuning (*LFD*) sensitivity coefficient. In fact, frequency shifts due to pressure fluctuations dominate in continuous wave (CW) operating machines, while frequency changes due to radiation pressure dominate in pulsed operating machines. It is imperative during the cavity course of design to reduce the frequency sensitivity coefficients to the minimum possible extent. In the case of SSR1, a CW operation was intended for the front end of PIP-II, therefore minimizing *df/dP* was of one of the design goals.

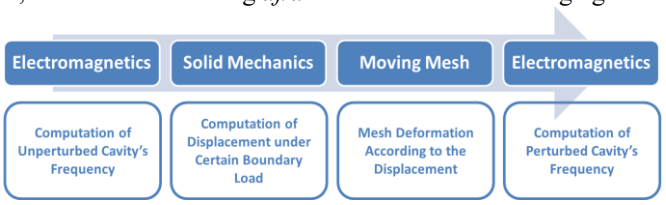

(a)

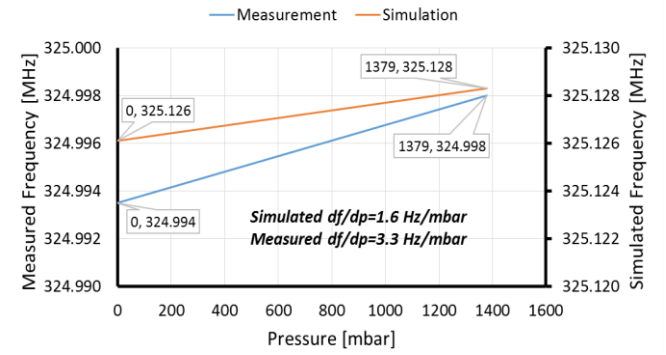

(c)

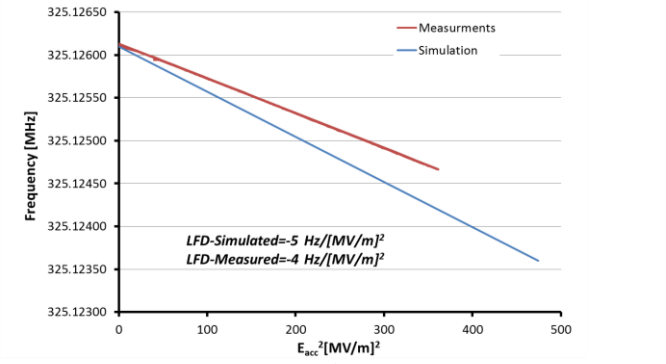

(d)

Fig. 14. Frequency detuning. (a) Modeling cycle of frequency detuning in SRF cavities. (b) Measured vs simulated frequency sensitivity to pressure (*df/dP*) in SSR1. (c) Measured vs simulated frequency sensitivity to radiation pressure (*LFD*) in SSR1.

Modeling of the detuning effects during cavity design requires multiphysics analyses, where the electromagnetic and mechanical aspects of the problem are coupled together [24]. Modeling the frequency detuning regardless of its source follows the scheme shown in Fig. 14(a), where the eigenmodes of the unperturbed cavity is computed first then the mechanical load, whether it is cryogenic pressure or radiation pressure is applied on the cavity and the displacement is found. The next step is to get the mesh deformed according to the calculated displacement and then re-compute the eigenmodes to find the amount of frequency shift.

Figure 14(b) and (c) compares the simulated versus measured values for *df/dP* and *LFD* for SSR1, respectively. Simulated values; *df/dP*=1.6 Hz/mbar, and *LFD*=-5 Hz/(MV/m)^2 are in good agreement with measured ones; *df/dP*=3.3 Hz/mbar, and *LFD*=-4 Hz/(MV/m)^2.

The sensitivity coefficient *df/dP* actually can have positive or negative sign depending on where most of the deformation is happening, whether it is in the high magnetic field or high electric field areas, respectively. Minimizing *df/dP* was accomplished by coupling the niobium cavity to the optimized helium vessel such that the structure produces deformation in the high electric and high magnetic field areas of equal amplitude but of opposite signs thus cancelling the effect of each other [25].

On the other hand, mechanical modes were computed for SSR1 and the lowest mechanical mode is found to be at 219 Hz, which is far from the 60 Hz electricity oscillation.

V. Fabrication and Quality Control

We explore in this section the fabrication process of the cavity ahead with the associated quality control practices.

a) Bare Cavity

As mentioned before, the cavity shell is fabricated from a high-purity niobium (Nb) sheets of 3 mm uniform thickness. All parts are formed and machined to follow exactly the RF domain shape, and joined by electron-beam welding. An exploded view of the SSR1 bare cavity is shown in Fig. 15(a) demonstrating its different constituents. The bare cavity consists of the shell, spoke pipe, two end walls, beam pipe, donut rib, daisy ribs, circumferential ribs, and coupler, vacuum, and beam pipe flanges. During the fabrication of the bare cavity, it was imperative to check the cavity's frequency before and after trimming the end walls to make sure that the frequency will end up within +1 MHz from the targeted 325 MHz goal to be reached for a cold jacketed SSR1.

Four flanges on the cavity, through which it interfaces with the helium vessel, are made of stainless steel connected to the niobium by means of copper-braze joints [26]. The grade of leak tightness and cleanliness of the flanged connections with the ultra-high vacuum RF volume was another subject of investigation in the design phase. The use of aluminum gaskets, high-silicon bronze set screws and stainless steel nuts were found to be the most reliable solution to seal the stainless steel flanged connections.

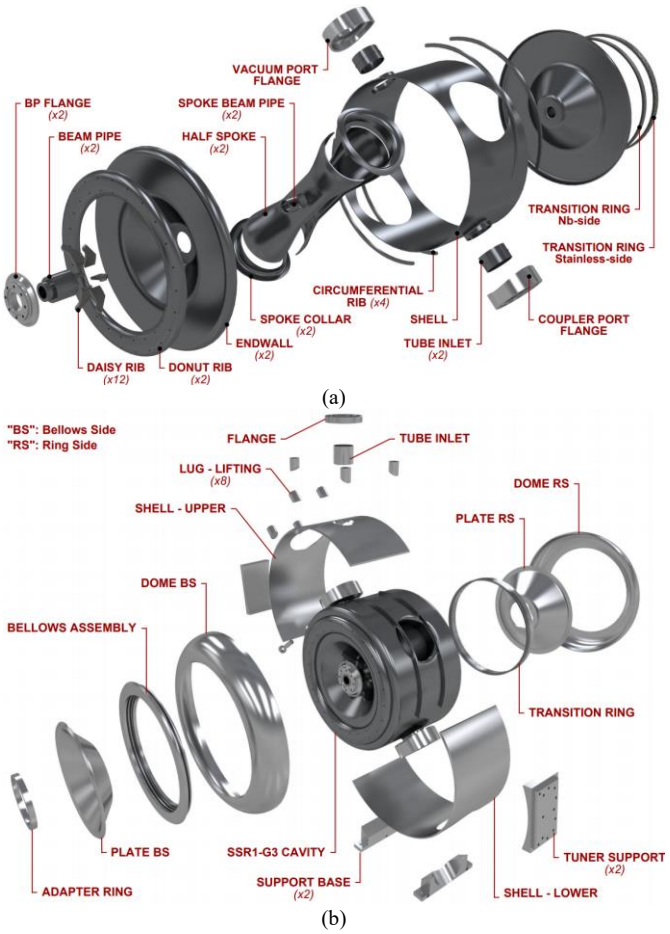

Fig. 15. Exploded view of SSR1 cavity. (a) Bare niobium cavity. (b) Stainless steel helium vessel.

b) Jacketed Cavity

The jacketed SSR1 cavity consists of two nested cryogenic pressure vessels: the inner vessel is the SSR1 bare cavity, and the outermost vessel is the helium containment (or helium) vessel, as shown in the exploded view of Fig. 15(b). The helium vessel is entirely made of 6.25 mm thick 316L stainless steel, which has quite neutral magnetic properties.

In fact, residual magnetic field can degrade the performance of SRF cavities affecting the quality factor. The helium vessel is assembled around the bare cavity by full penetration tungsten inert gas (TIG) welds. all vessel components must be electro-polished before welding to guarantee the cleanliness of the process. All welds joining the stainless-steel vessel are performed following the ASME Code.

Three subassemblies are pre-welded, specifically; shell, plate, and bellow subassemblies. The shell subassembly is then divided into two parts that will go for dry fit around the bare cavity. Once all sub-assemblies are ready, a dry fit is performed. Any additional machining is done at this stage to make sure that the dry-fit is successful. Tack welds are then used to keep component in place after having aligned all vessel parts with cavity's beam pipe ports and side ports.

The temperature of the resonator inner surface is monitored by thermal camera and is kept ≤ 75 °C at any time during the welding process, regardless of the nature of the purging gas.

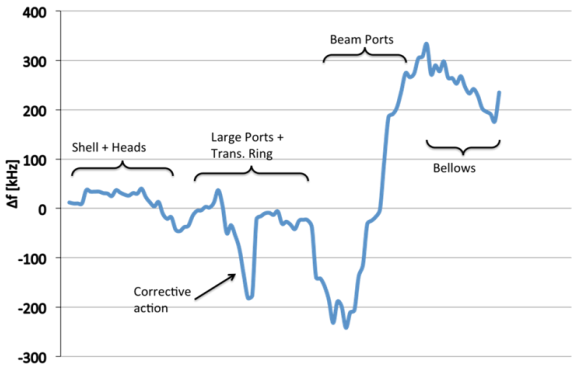

Fig. 16. Frequency change during welding of the helium vessel for SSR1 cavity.

Table 6. Mechanical Requirments on SSR1.

#	Weld	Freq Shift [kHz]	Critical
1	Tring	-90	No
2	Shell	-2	No
3	CP-VP	-238	Yes
4	BP Tring side	294	Yes
5	BP bellows side	35	No
6	Bellows	-121	Yes

Moreover, the resonant frequency of the resonator is measured at regular intervals to control the welding process and avoid putting excessive strain on the resonator because of the thermal shrinkage. Figure 16 shows the change in measured frequency of SSR1-107 for instance. The maximum change in frequency (200 kHz) happens during the weld of the side ports. The entire welding process must not change the resonant frequency more than 300 kHz, as larger frequency changes will be difficult to mitigate by inelastic tuning.

The inevitable weld shrinkage on the vessel comprising parts due to the relatively heavy TIG welds should be guided in such a way to avoid squeezing the resonator. Moreover, the welding process must follow a certain sequence. The weld sequence, as indicated in Fig. 16, is critical to minimize the thermal stresses on the resonator. After the completion of welding, final machining of tuner support, cavity support and lifting lugs is made.

Table 6 shows the frequency shift of the different welds in sequence averaged over the ten dressed cavities and demonstrate the criticality of each weld. As shown in the table, the critical welds are; coupler and vacuum port (weld #3), beam pipe weld on transition ring side (weld #4), and the bellow assembly (weld #6). The most critical weld exhibiting the largest frequency shift of +294 kHz is weld #4. The reason behind this is that the transition ring side of the cavity is quite stiff, consequently, all the deformation is taking place at the beam pipe stretching the gap on the that side by approximately 500 μm.

VI. Tuning, Preparation and Processing

In this section, we describe the process of tuning, preparing and chemical processing SSR1 cavities before testing.

a) Frequency Inelastic Tuning

During cavity production, it is necessary to set frequency goals throughout the entire process to match the final target frequency of 325 MHz for a cold jacketed SSR1. The bare cavity received from the vendor has typically a resonant frequency of 325.6 (±0.2) MHz. The average frequency shift for bare SSR1 cavity due to the leak check is -80 kHz. The bulk BCP removes 150 µm on average from the cavity surface, while the light chemical processing results in 30 µm material removal. For both processes the frequency variation is not negligible, the frequency shift produced by the bulk BCP has been averaged over 10 cavities to be -150 kHz, while the one due to light BCP is -30 kHz. Transition ring and helium vessel welding causes frequency change as well.

The total inelastic frequency tuning needed for bare cavity is approximately 1 MHz. Considering the cavity sensitivity of 540 kHz/mm and its spring constant of 23 kN/mm, the tuning requires a robust fixture capable of delivering up to 40 kN.

Figure 17(a) shows the tuning fixture we have used to tune SSR1 cavities [27]. It consists of a box equipped with two threaded rods to be connected to the cavity's beam pipes providing the needed pushing or pulling force. Two load cells are used to measure the forces applied on each rod, while four displacement gauges are used to measure the displacement of the cavity's end walls. A set of antennae is mounted on the coupler ports to allow measuring the cavity's resonance frequency step by step during the tuning process.

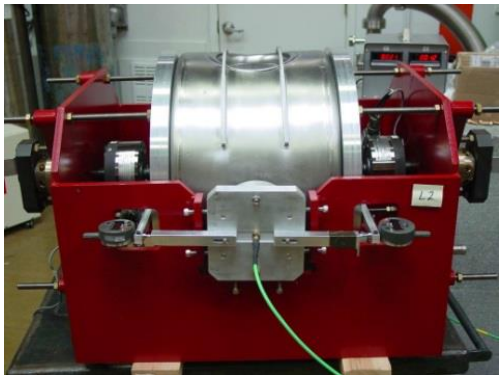

(a)

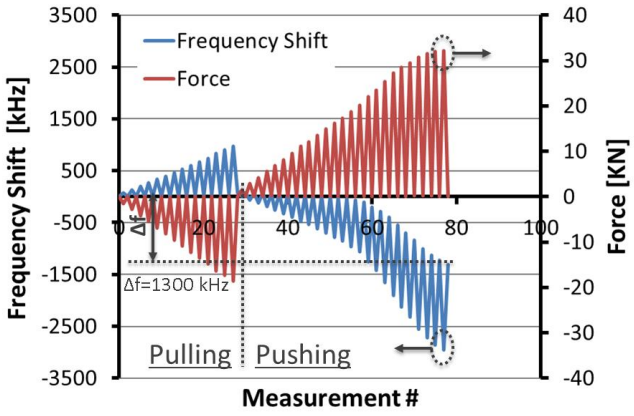

(b)

Fig. 17. Inelastic tuning of SSR1 cavity. (a) Tuning fixture. (b) SSR1-112 frequency and applied forced during inelastic tuning.

Figure 17(b) shows the resonance frequency of SSR1-112 during the tuning. One can see how for small forces applied the process is reversible and the frequency in the relaxed state is equal to the one before pushing or pulling. When the force overcomes the elastic limit of the material the cavity starts yielding at approximately 13 kN, which corresponds to 600 kHz shift under force, and as result the frequency for the relaxed cavity changes. We start by pulling the cavity increasing its frequency slightly to harden the cavity material as we will be using a pushing tuner. Afterwards we apply compression force to bring the cavity to a lower warm targeted frequency value (324.6 MHz), as can be seen in Fig. 17(b), for cavity #112, which we started tuning it from a frequency value of 325.9. After the initial pulling for hardening purposes, we compressed the cavity in small steps where we repeatedly apply then release force and monitor the frequency shift. A total of -1300 kHz is obtained for this cavity.

b) Preparation and Chemical Processing

SSR1 resonators undergo a series of operations involving cleaning, acid-etching and baking (see Table 7). The baseline recipe is aimed to obtain the best performance in the VTS (Vertical Test Stand). Initially, resonators need to be cleaned to remove any residue left by the manufacturing process. This is done by degreasing all surfaces in an ultrasonic tank followed by a thorough rinsing with ultra-pure water. Next, a layer of about 120-150 µm is removed with a buffered-chemical processing solution (bulk BCP). This is achieved through two sub-cycles interposed with a rotation of 180 degrees to improve uniformity. After another cycle of degreasing and rinsing, resonators are subject to a high-pressure-rinse (HPR) with a tool having a vertical water wand.

Subsequently, resonators are baked at 600 °C with a 10-hour plateau and a climb rate of less than 5 °C/min. This is referred to as hydrogen-degassing and serves the purpose of reducing the onset of Q-disease.

After an intermediate step of RF measurements and frequency tuning, resonators are again degreased and rinsed and routed for a second cycle of chemistry only removing 20-30 µm this time (light BCP). After another cycle of degreasing and rinsing, the resonator is subject to a thorough HPR performed on two different tools, one having the pressure wand in the vertical position, the other in the horizontal position. Utilizing both tools on the same resonator has been shown to improve the performance in the cold tests in terms of field emission (FE).

Finally, resonators are evacuated, leak-checked to 10^{-10} mbar-l/s or better and baked under vacuum at 120 °C for a

Table 7. Preparation steps of SSR1 cavities for cold test

#	Operation	Details
1	Bulk BCP	2x(60-75) µm
2	HPR	Vertical
3	Heat Treatment	600 ºC, 10 h
4	Light BCP	20-30 µm
5	HPR	Vertical+Horizontal
6	Leak Check	$<10^{-10}$ mbar-l/s
7	Low-T Bake	120 ºC, 48 h

minimum of 24 hours. This helps substantially in reducing the time necessary for processing through multipacting barriers which SSR1 resonators are known to suffer from. After the transition ring and the helium vessel are welded onto the qualified resonators, an additional cycle of light BCP and HPR is performed.

VII. Testing and Qualification

To date 10 bare SSR1 cavities have been fabricated and tested at 2 K in the vertical test stand. All of them has shown performance meeting PIP-II requirements [12-13], so they were jacketed with helium vessel.

Cold tests of bare SSR1 cavities are performed in the vertical test stand (VTS) cryostat. Cavities are connected to the vacuum pump, but usually are not actively pumped during tests. Cavities are instrumented with Oscillating Superleak second-sound Transducers (OST) to detect second sound emitted by a quench [28]. OSTs are positioned close to the spoke-to-sidewall transition area, near the maximum magnetic field region, where the quench is most likely to happen.

Figure 18 shows the results of the cold test for 10 spoke cavities tested to date demonstrating the quality factor versus gradient for each cavity and indicating PIP-II requirements (in green). Table 8 summarizes the cold test of SSR1 bare cavities at VTS indicating their unloaded quality factor (Q_0) at PIP-II gradient, maximum gradient and level of radiation for each cavity at their last test. Maximum achieved gradient in these cavities is in the range from 17 to 22 MV/m and it is limited by quench in all cavities but 112.

Cavity #112 had strong MP at 6.5 MV/m. It temporarily reached 17 MV/m at 4.4 K, but when the input power level was decreased, the accelerating gradient dropped back to the 6.5 MV/m MP barrier. Subsequent conditioning at 100-120 W of input power for more than 10 hours did not clean MP and it was not possible to increase field in the cavity above 6.5 MV/m. At 2 K and Eacc =6.5 MV/m, we measured quality factor Q_0=1.2x10^{10}, which is comparable to other qualified cavities at the same field level. Since this cavity showed potentially good performance and we did not find any performance degradation associated with manufacturing, we conditionally qualified this cavity for PIP-II.

OST system detected quench signals near the spoke to sidewall transition area in four cavities. In one test, OST signals were not detected during quench and we conclude that the area of the quench in this case is on the cavity end-wall. Four cavities (105, 108, 112 and 113) show very little radiation, while three other cavities (107, 109 and 110) have FE onset at 10, 13 and 17 MV/m at their first test. Cavities will receive additional light BCP (20–30 μm) and HPR post jacketing. We expect that additional processing and HPR will reduce the level of FE in cavities 107, 109 and 110. The 10 qualified bare cavities 105-114 were jacketed following the procedure explained earlier.

The jacketed cavities have demonstrated very promising performance in terms of sensitivity to He-pressure fluctuations (*df/dP).* Table 9 summarizes the data for *df/dP* frequency sensitivity coefficient measured during leak check of jacketed cavities. The average measured *df/dP* of jacketed cavities is 3.6 Hz/mbar, which is very small and is indicating that SSR1 cavities are quite insensitive to pressure. The variation in the measured *df/dP* among the 10 dressed cavities are mainly caused by fabrication tolerances and small variations in welding vessels to bare cavities.

Performance of the first jacketed SSR1 (#107) was evaluated during tests in the spoke test stand (STC) [29]. Testing in STC resembles the actual cryomodule environment where the cavity is over-coupled and an actual tuner and a high-power coupler are attached to it, as shown in Fig. 19(a). The STC results in Fig. 19(b) demonstrates quality factor versus gradient for the testing of 107 in both STC and VTS compared to PIP-II requirements.

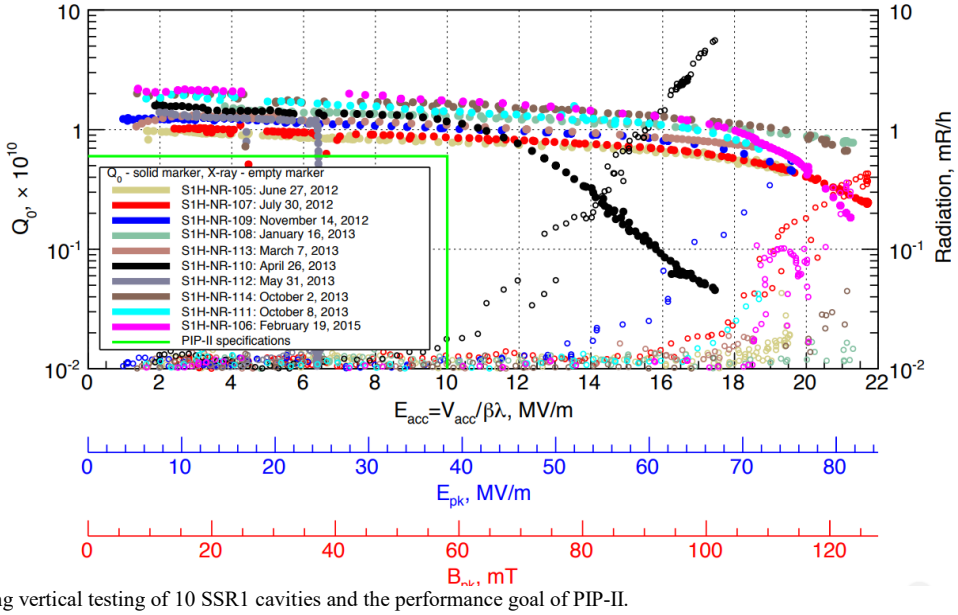

Fig. 18. Q_0 vs E_{acc} during vertical testing of 10 SSR1 cavities and the performance goal of PIP-II.

Table 8. Summary of the cold test results of SSR1 at VTS

Cavity Serial #	Q_0 (12MV/m), x10^{10}	*Max Eacc* [MV/m]	*Radiation at Max Eacc* [Mr/h]
105	0.8	20	<0.1
106	1.7	21	0.3
107	0.9	22	0.4
108	1.3	21	<0.1
109	1.0	20	0.5
110	1.1	18	5
111	1.4	19	<0.1
112*	1.2	17*	<0.1
113	1.1	19	<0.1
114	1.6	21	<0.1

*Cavity #112 was conditionally qualified since it had strong multipactor at 6.5 MV/m. It temporarily reached 17 MV/m at 4.4K, but when the input power level was decreased, the accelerating gradient dropped back to the 6.5 MV/m MP barrier.

Table 9. Frequency sensitivity to pressure (*df/dP*) in Hz/mbar for the the ten jacketed SSR1 cavities without tuners

Cavity Serial #	*df/dP [Hz/mbar]* (jacketed cavity at 293K w/o tuner)
105	~0
106	~0
107	6
108	-0.9
109	4.1
110	5.9
111	2.0
112	6.8
113	4.7
114	7.5

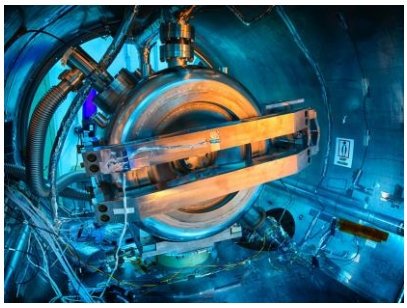

(a)

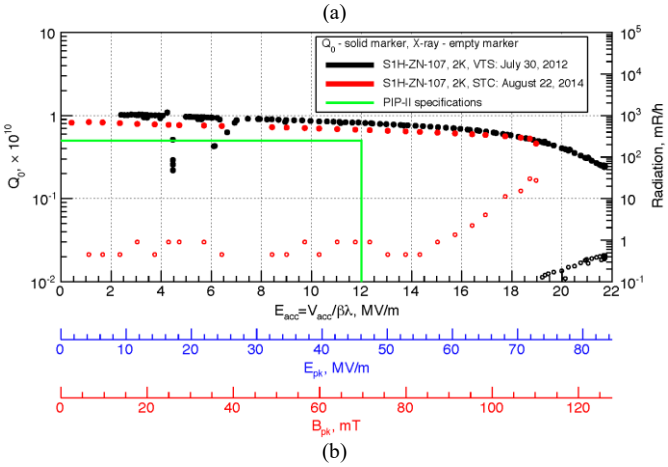

(b)

Fig. 19. Integrated test of SSR1-107 in the Spoke Test Stand (STC). (a) Picture of the cavity inside STC. (b) Q_0 vs E_{acc} curve showing that the cavity exceeded the performance goals of PIP-II.

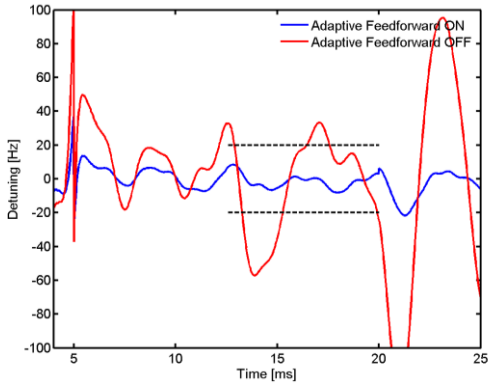

Fig. 20. Cavity Detuning during pulsed operation at 12 MV/m, 20 Hz repetition rate, with a rise time of 12.5 ms, flat top of 7.5 ms, and gentle emptying. Flat top was longer than expected for PIP-II for diagnostic purposes.

The STC results fulfill the specifications of the project from the RF and mechanical perspectives. The Q_0 vs. E_{acc} profile measured for the jacketed cavity (in STC) matches the one of the bare cavity (in Vertical Test Stand). This indicates that the jacketing (welding) process has not degraded the performance of the niobium bare cavity.

Meanwhile, the frequency sensitivity to pressure coefficient *df/dP* was measured in the integrated test of 107 at STC, while having the coupler and tuner attached to the cavity. After cooling down to 2 K, the measured *df/dP* is 3 Hz/mbar, which is far below the specification of the PIP-II project and validate the design approach of SSR1's helium vessel.

Since PIP-II presents a unique challenge with respect to resonance stability, active resonance stabilization was investigated. The combination of low beam-loading and high Q gives an unusually narrow half bandwidth (45 Hz), setting a tight tolerance on the allowable microphonics environment. Additionally, the machine will be operated in a 20 Hz pulsed mode which introduces significant additional mechanical disturbance to the cavity during operation. To ensure stable operation, PIP-II will require fast, active resonance stabilization via the piezo tuners installed on all cavities.

Active compensation techniques developed for the PIP-II SSR1 cavity included feedforward compensation of the cavity's Lorentz Force Detuning [30], proportional feedback in CW operation [31], and pulsed compensation using an Adaptive Feedforward technique developed at FNAL [32-33]. This technique uses a set of training piezo pulses to characterize the cavity system response, then calculates a proper compensation piezo voltage signal, updated on a pulse to pulse basis, to compensate for the deterministic detuning. The results of this detuning can be seen in Fig. 20. Without the active compensation, the detuning is more than 100 Hz, exceeding PIP-II requirements of 20 Hz [3]. The developed active compensation mechanism successfully reduces the detuning to less than the required 20 Hz.

VIII. Conclusion

Spoke cavities are one of the essential components for the front end of SRF proton accelerators. Spoke cavities can be conveniently designed in the β range of 0.1-0.5. Diverse

engineering effort from RF to mechanical and thermal fronts is needed to realize those spoke cavities.

A single spoke cavity was designed for PIP-II project at Fermilab. Design of the cavity addressed PIP-II requirements from RF and mechanical aspects. Analyses of multipacting, HOMs, kick, multipole effect were carried out to address any issue during the RF design stage of the cavity. Structural analysis was performed to guarantee that the cavity structure can handle the 4 bar maximum allowable pressure at 2 K. Meanwhile, optimization of the helium vessel was done to minimize the frequency sensitivity to He pressure fluctuations *df/dP*.

A total of 10 bare SSR1 cavities have been fabricated from high-purity niobium (Nb) sheets. All parts are formed and machined to follow exactly the RF domain shape, and joined by electron-beam welding. All the bare cavities were qualified at the vertical test stand (critically coupled test). Several multipacting barriers were encountered during testing as predicted by simulation. Proper 120 °C baking for at least 48 hours helps to reduce the conditioning process. Cavities are then jacketed in stainless steel helium vessels. Monitoring the cavity frequency during fabrication is essential to meet the 325 MHz frequency goal at 2 K.

An integrated test to the jacketed cavity (overcoupled) with the high-power coupler and the tuner attached is needed and was performed to test the integrated cavity systems and qualify the cavity for string assembly. Development SSR1 cavities is progressing steadily towards assembling the first SSR1 cryomodule by 2019.

ACKNOWLEDGMENT

Authors are grateful to the personnel of the Fermilab Argonne joint processing facility and the Fermilab Technical Division SRF Development and Test & Instrumentation departments for their hard work in preparing SSR1 cavities for cold tests. We also acknowledge the engineering and technical staff of the Fermilab's Accelerator and Technical Divisions for the successful upgrade of the STC to 2 K operation.

Bare cavities were fabricated by C. F. Roark Welding & Engineering Co. Inc., while cavities got jacketed at Meyer Tool &Mfg.

REFERENCES

[1] https://pip2.fnal.gov/

[2] P. Derwent, S. Holmes, and V. Lebedev, "An 800 MeV superconducting Linac to support Megawatt proton operation at Fermilab," *proceedings of Linac14,* Geneva, Switzerland, 2014.

[3] M. Ball, A. Burov, B. Chase, A. Chakravarty, A. Chen et al., "The PIP-II conceptual design report," July 2017.

[4] P. N. Ostroumov, B. Mustapha, Z. A. Conway, R. L. Fischer, S. Gerbick, M. Kedzie, M. P. Kelly, I. V. Gonin, and S. Nagaitsev, "Development of a half-wave resonator for Project X," *proceedings of IPAC12*, New Orleans, USA, 2012.

[5] L. Ristori, M. Awida, I. Gonin, M. Merio, D. Passarelli, and V. Yakovlev, "Design of SSR1 spoke resonators for PXIE," *proceedings of IPAC12*, New Orleans, USA, 2012.

[6] S. Kim, "SNS superconducting LINAC operational experience and upgrade path," *proceedings of LINAC08,* Victoria, BC, Canada, 2008.

[7] M. Leitner, B. Bird, F. Casagrande, S. Chouhan, C. Compton, J. Crisp, K. Elliot et al. "The FRIB project at MSU," *proceedings of SRF13*, Paris, France, 2013.

[8] V. Zvyagintsev, K. Fong, M. Laverty, R. E. Laxdal, A. K. Mitra, T. Ries, and I. Sekachev, "Results and experience with single cavity tests of medium beta superconducting quarter wave resonators at TRIUMF," *proceedings of EPAC06,* Edinburgh, UK, 2006.

[9] CST Microwave Studio v 2013.

[10] G. Romanov "Simulation of multipacting in HINS accelerating structures with CST Particle Studio," *proceedings of LINAC08*, Victoria, BC, Canada, 2008.

[11] P. Berrutti, T. Khabiboulline, L. Ristori, G. Romanov, A. Sukhanov, and V. Yakovlev, "Multipacting simulations of SSR2 cavity at FNAL," *proceedings of IPAC15*, Richmond, VA, USA, 2015.

[12] A. Sukhanov, M. Awida, P. Berrutti, C. Ginsburg, T. Khbiboulline et. al, "Cold tests of SSR1 resonators for PXIE," *proceedings of SRF13*, Paris, France, 2013.

[13] A. Sukhanov, M. Awida, P. Berrutti, E. Cullerton, B. Hanna et al., "Result of cold tests of the Fermilab SSR1 cavities," *proceedings of Linac14*, Geneva, Switzerland, 2014.

[14] M. Awida, I. Gonin, P. Berrutti, T. Khabiboulline, and V. Yakovlev, "SSR1 HOM analysis and measurements," *proceedings of IPAC12*, New Orleans, USA, 2012.

[15] T. Khabiboulline, A. Sukhanov, M. Awida, I. Gonin, A. Lunin et al., "Resonance excitation of longitudinal High Order Modes in Project X Linac," *proceedings of IPAC12*, New Orleans, USA, 2012.

[16] M. Awida, I. Gonin, P. Berrutti, T. Khabiboulline, and V. Yakovlev, "Transverse kick analysis of SSR1 due to possible variations in fabrication," *proceedings of IPAC12*, New Orleans, USA, 2012.

[17] P. Berrutti, T. Khabiboulline, V. Lebedev, and V. Yakovlev, "Transverse field perturbation for PIP-II SRF cavities," *proceedings of IPAC15*, Richmond, VA, USA, 2015.

[18] D. Passarelli, R. Wands, M. Merio, and L. Ristori, "Methodology for the structural design of single spoke accelerating cavities at Fermilab", in *Nuclear Instruments and Methods in Physics Research Section A*, vol. 834C, pp. 1-9, 2016.

[19] Ansys user guide v 2014.

[20] S. Kazakov, B. Hanna, and O. Pronitchev, "Testing of 325 MHz couplers at test stand in resonance mode," *proceedings of SRF15*, Whistler, BC, Canada, 2015.

[21] O. Pronitchev, and S. Kazakov, "Mechanical design of a high power coupler for the PIP-II 325 MHz SSR1 RF cavity," *proceedings of SRF15*, Whistler, BC, Canada, 2015.

[22] D. Passarelli, and L. Ristori. "SSR1 tuner mechanism: passive and active device," *proceedings of Linac14*, Geneva, Switzerland, 2014.

[23] H. Padamsee, J. Knobloch, and T. Hays, "RF superconductivity for accelerators," John Wiley, New York 2008.

[24] M. H. Awida, I. Gonin, D. Passarelli, A. Sukanov, T. Khabiboulline, and V. Yakovlev, "Multiphysics analysis of frequency detuning in superconducting RF cavities for proton particle accelerators," In 2015 IEEE MTT-S International Conference on Numerical Electromagnetic and Multiphysics Modeling and Optimization (NEMO), pp. 1-3. IEEE, 2015.

[25] D. Passarelli, M. H. Awida, I. V. Gonin, L. Ristori, and V. Yakovlev, "Pressure sensitivity characterization of superconducting spoke cavities," *proceedings of IPAC12*, New Orleans, USA, 2012.

[26] L. Ristori, and W. Toter, "Development at ANL of a copper-brazed joint for the coupling of the niobium cavity end-wall to the stainless steel helium vessel in the Fermilab SSR1 resonator," *proceedings of IPAC12*, New Orleans, USA, 2012.

[27] P. Berrutti, M. Awida,T. Khabiboulline, D. Passarelli, L. Ristori, and V. Yakovlev, "Tuning process of SSR1 cavity for Project X at FNAL," *proceedings of PAC13,* Pasadena, CA, USA, 2013.

[28] Y. Maximenko, and D. Segatskov, "Quench dynamics in SRF cavities: can we locate the quench origin with 2nd sound?," *proceedings of PAC11*, New York, USA, 2011.

[29] A. Hocker, E. Cullerton, B. Hanna, W. Schappert and A. Sukhanov, "RF tests of dressed 325 MHz single-spoke resonators at 2K," *proceedings of Linac14*, Geneva, Switzerland, 2014.

[30] W. Schappert, "Resonance control for future accelerators," *Proceedings of LINAC16*, East Lansing, MI, TU2A04

[31] W. Schappert, J. Holzbauer, Y. Pichalnikov, "Progress of FNAL in the field of the active resonance control for narrow bandwidth SRF cavities" *Proceedings of IPAC15*, Richmond, VA, USA, 2015.
[32] W.Schappert, Y. Pischanikov "Adaptive compensation for Lorentz force detuning in superconducting RF cavities," *proceedings of SRF2011*, Chicago, USA, 2011.
[33] Pischalnikov, W.Schappert, "Adaptive LFD Compensation" Fermilab Preprint-TM2476-TD.